Interaction of Glutathione Reductase with Heavy Metal: The Binding of Hg(II) or Cd(II) to the Reduced Enzyme Affects Both the Redox Dithiol Pair and the Flavin

Thierry Picaud and Alain Desbois*

Département de Biologie Joliot-Curie, Service de Biophysique des Fonctions Membranaires, Commissariat à l'Energie Atomique (CEA) and Unité de Recherche Associée au Centre National de la Recherche Scientifique (URA CNRS 2096), CEA/Saclay, F-91191 Gif-sur-Yvette Cedex, France

Received June 29, 2006; Revised Manuscript Received September 29, 2006

ABSTRACT: To determine the inhibition mechanism of yeast glutathione reductase (GR) by heavy metal, we have compared the electronic absorption and resonance Raman (RR) spectra of the enzyme in its oxidized (E_{ox}) and two-electron reduced (EH_2) forms, in the absence and the presence of Hg(II) or Cd(II). The spectral data clearly show a redox dependence of the metal binding. The metal ions do not affect the absorption and RR spectra of E_{ox}. On the contrary, the EH_2 spectra, generated by addition of NADPH, are strongly modified by the presence of heavy metal. The absorption changes of EH_2 are metal-dependent. On the one hand, the main flavin band observed at 450 nm for EH_2 is red-shifted at 455 nm for the EH_2−Hg(II) complex and at 451 nm for the EH_2−Cd(II) complex. On the other hand, the characteristic charge-transfer (CT) band at 540 nm is quenched upon metal binding to EH_2. In NADPH excess, a new CT band is observed at 610 nm for the EH_2−Hg(II)−NADPH complex and at 590 nm for EH_2−Cd-(II)−NADPH. The RR spectra of the EH_2−metal complexes are not sensitive to the NADPH concentration. With reference to the RR spectra of EH_2 in which the frequencies of bands II and III were observed at 1582 and 1547 cm^{-1}, respectively, those of the EH_2−metal complexes are detected at 1577 and 1542 cm^{-1}, indicating an increased flavin bending upon metal coordination to EH_2. From the frequency shifts of band III, a concomitant weakening of the H-bonding state of the N_5 atom is also deduced. Taking into account the different chemical properties of Hg(II) and Cd(II), the coordination number of the bound metal ion was deduced to be different in GR. A mechanism of the GR inhibition is proposed. It proceeds primarily by a specific binding of the metal to the redox thiol/thiolate pair and the catalytic histidine of EH_2. The bound metal ion then acts on the bending of the isoalloxazine ring of FAD as well as on the hydrophobicity of its microenvironment.

Heavy metals, and particularly Cd and Hg, are highly toxic to most biological organisms and represent a source of major problems for the environment as well as the public health. The extent of the toxic effects depends on the chemical form of the metal species. Heavy metals generally cause oxidative stress, shifting the redox balance toward an oxidizing milieu (*1*−*3*). The redox cycling of glutathione is central to the cellular response to oxidative stress. With intracellular concentrations of reduced glutathione (GSH)[1] varying from 1 to 10 mM (*4*, *5*), this low molecular weight molecule is the most abundant thiol-containing compound in living cells and protects cells against various oxidants, free radicals, and cytotoxic agents. Glutathione reductase (GR, EC 1.6.4.2, NADPH: oxidized-glutathione oxidoreductase) is a key enzyme in the maintenance of a cytosolic GSH/ glutathione disulfide (GSSG) ratio equal to or higher than 100. This flavoprotein belongs to the pyridine nucleotide disulfide oxidoreductase family and shares many structural and spectroscopic similarities with other members of this family such as lipoamide dehydrogenase, thioredoxin reductase, and mercuric ion reductase (*6*). GR is a homodimer in which each monomer contains a flavin adenine dinucleotide (FAD) cofactor sandwiched between the pyridine nucleotide binding site and a redox-active disulfide group (Cys45/Cys50 in yeast GR) (*7*−*10*). The reaction catalyzed by GR is the reduction of GSSG by NADPH.

$$GSSG + NADPH + H^+ \Leftrightarrow 2\,GSH + NADP^+ \quad (1)$$

This global reaction can be subdivided into two half-reactions (*11*). The first one is reductive with the reduction of oxidized GR (E_{ox}) by NADPH. This step gives rise to the formation of a two-electron reduced species (EH_2) with an oxidized FAD and a reduced dithiol center.

$$E_{ox} + NADPH + H^+ \Leftrightarrow EH_2 + NADP^+ \quad (2)$$

The second half-reaction reaction is oxidative. EH_2 reacts with GSSG, yielding two molecules of GSH and regenerating the oxidized enzyme with its active disulfide site. In this reaction, a stable mixed disulfide (MDS) intermediate is formed.

* Corresponding author. Telephone: 33-1-69-08-37-22. Fax: 33-1-69-08-91-11. E-mail: alain.desbois@cea.fr.

[1] Abbreviations: GR, glutathione reductase; GSH, reduced glutathione; GSSG, glutathione disulfide; E_{ox}, oxidized GR; EH_2, two-electron reduced GR; EH_4, four-electron reduced GR; MDS, mixed disulfide; RR, resonance Raman; CT, charge transfer; CCD, charge-coupled device.

10.1021/bi061304m CCC: $33.50
Published on Web 12/05/2006

$$EH_2 + GSSG \Leftrightarrow EH_2{-}GSSG \Leftrightarrow MDS{-}GSH \Leftrightarrow MDS + GSH \quad (3)$$

$$MDS \Leftrightarrow E_{ox} - GSH \Leftrightarrow E_{ox} + GSH \quad (4)$$

Various heavy metals inactivate GR (*12*−*14*). These data suggest that the redox cysteine pair is affected by the metal insertion. However, the molecular mechanism of inhibition by these metal ions remains to be determined. Recent studies using resonance Raman (RR) spectroscopy showed the mutual influences of the two redox centers of GR in different oxidation states (*15*, *16*). In the present study, we have investigated the absorption and RR spectra of the enzyme in the E_{ox} and EH_2 states, in the absence or the presence of either Hg(II) or Cd(II). Our results highlight the importance of both the reduced dithiol center and the conformation and microenvironment of the isoalloxazine ring in the inactivation of the functional EH_2 form of GR.

EXPERIMENTAL PROCEDURES

Protein Preparation. Yeast GR was purchased from Sigma and purified as previously described (*16*). The enzyme concentration was expressed as the concentration of enzyme-bound FAD using the extinction coefficient 11 300 M^{-1} cm^{-1} at 462 nm (*17*). It was in the ranges (2.3−2.8) × 10^{-5} and (3.0−3.5) × 10^{-4} M for the absorption and RR experiments, respectively. The NADPH concentration was calculated using ϵ_{340} = 6220 M^{-1} cm^{-1}. NADPH, $HgCl_2$, and $CdCl_2$ were purchased from Sigma. All other chemicals were of the highest grade commercially available.

The EH_2 form of the enzyme was generated by anaerobic reduction of oxidized GR with NADPH (*15*, *16*). After equilibration of E_{ox} under a wet atmosphere of argon, a small aliquot of concentrated $HgCl_2$ or $CdCl_2$ was anaerobically added. This mixture was then titrated with various concentrations of NADPH under wet argon (*16*). We also performed a series of experiments in which GR was first anaerobically reduced by NADPH and then titrated by the metal ion. For given concentrations of NADPH and metal ion, the order of addition of the two reactants has no influence on the final spectra. Because GSH is expected to strongly sequester most of the Hg(II) or Cd(II) ions added (*18*, *19*), the effects of the metal ions on the GSH-reduced enzyme were not investigated.

Spectroscopies. Electronic absorption spectra were recorded using a UV−vis Varian Cary5E spectrophotometer. Resonance Raman spectra were obtained using a Jobin-Yvon U1000 spectrometer equipped with an N_2-cooled CCD detector (Spectrum one, Jobin-Yvon, France) (*20*). The spectra were excited with the 441.6 nm line of a He/Cd laser (Liconix, model 4050) or the 363.8 nm line of an Ar laser (Coherent, model Innova 100). The signal-to-noise ratios were improved by spectral collections using a 30 s accumulation time. The spectral analysis was made using the Grams 32 software (Galactic Industries) and methods previously described (*16*, *20*). The frequency precision was 0.5−1 cm^{-1} for the most intense RR bands and 1.5−2 cm^{-1} for the weakest bands. All the spectroscopic measurements were recorded at 20 ± 1 °C.

RESULTS

Electronic Absorption Spectra of GR in the Presence of Hg(II) or Cd(II). The influence of the metal ions on the electronic absorption spectra of oxidized and reduced GR is shown in Figures 1 and 2. The 350−700 nm regions of the spectra of oxidized GR (E_{ox}) at pH 7.4 are dominated by two broad $\pi \rightarrow \pi^*$ flavin transitions peaking at 378 and 462 nm. On each side of the 462 nm band, two marked shoulders are observed at 441 and 485 nm. The addition of up to 10 mol equiv/FAD of Hg(II) or Cd(II) does not significantly affect the absorption spectrum of E_{ox} (Figure 1a, data not shown). The absorption spectrum of the EH_2 form shows a main flavin band at 450 nm with two shoulders at 432 and 479 nm (Table 1). In the green region, a broad band at 540 nm is characteristic of a CT complex between the thiolate group of the conserved proximal Cys (Cys50 in yeast GR) and the oxidized flavin (*21*, *22*, this work). When an excess of NADPH is present, EH_2 forms a complex with NADPH (EH_2−NADPH), which further increases the absorbance at 540 nm (*22*, this work). In the presence of Hg(II) (1.5−5 equiv/FAD), the reduction of E_{ox} by NADPH produces a main flavin band at 455 nm (Figure 1, Table 1). When compared to the main flavin transition of EH_2, that of the EH_2−Hg(II) complex is therefore red-shifted by 5 nm. Moreover, we observe no CT transition at 540 nm for the EH_2−Hg(II) complex (Figure 1, Table 1). Finally, a broad long-wavelength absorption grows at 610 nm when the concentration of free NADPH is increased (Figures 1 and

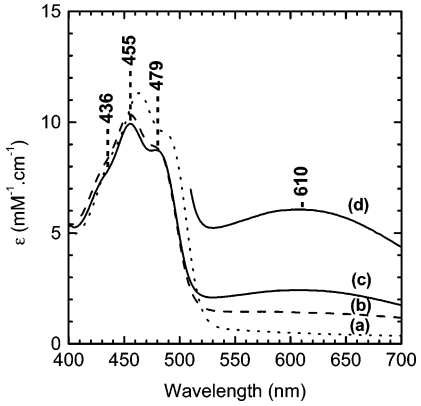

FIGURE 1: Electronic absorption spectra of yeast GR in the presence of 1.5 equiv/FAD of Hg(II) at pH 7.2. (A) Oxidized GR. (B) GR reduced with 3 equiv/FAD of NADPH. (C) GR reduced with 7 equiv/FAD of NADPH. (d) 510−700 nm region of spectrum C multiplied by a factor of 2.5.

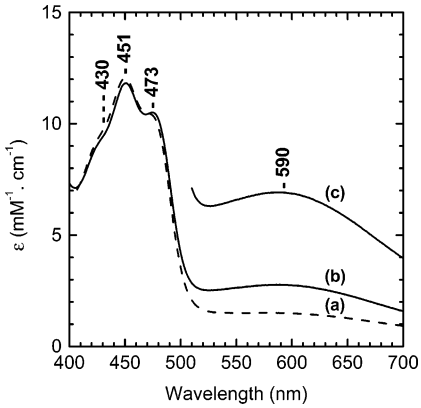

FIGURE 2: Electronic absorption spectra of yeast GR in the presence of 4.5 equiv/FAD of Cd(II) at pH 7.2. (A) GR reduced with 3 equiv/FAD of NADPH. (B) GR reduced with 8 equiv/FAD of NADPH. (C) 510−700 nm region of spectrum B multiplied by a factor of 2.5.

Table 1: Observed Absorption Maxima (nm) of Oxidized (E_{ox}) and NADPH-Reduced (EH_2) GR in the Absence or the Presence of Hg(II) or Cd(II)

GR		λ_{max} flavin		λ_{max} CT
$E_{ox} \pm$ Hg(II) $E_{ox} \pm$ Cd(II))	441 (sh)[a]	462	485 (sh)	
EH_2 EH_2-NADPH	432 (sh)	450	479 (sh)	540
EH_2-Hg(II)	436 (sh)	455	478 (sh)	
EH_2-Hg(II)$-$NADPH	436 (sh)	455	479 (sh)	610
EH_2-Cd(II)	429 (sh)	451	472 (sh)	
EH_2-Cd(II)$-$NADPH	430 (sh)	451	473 (sh)	590

[a] sh indicates shoulder.

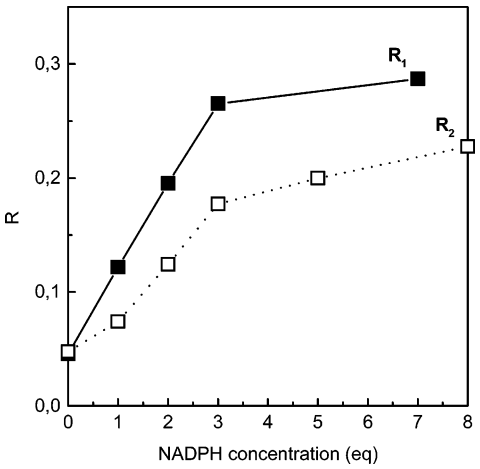

FIGURE 3: Variation of the R_1 and R_2 ratios as a function of the NADPH concentration (in equiv/FAD). R_1 corresponds to the NADPH-reduced enzyme in the presence of 1.5 equiv/FAD of Hg-(II) and represents the intensity ratio of the 610 nm CT band and the 455 nm flavin band. R_2 corresponds to the NADPH-reduced enzyme in the presence of 4.5 equiv/FAD of Cd(II) and is the intensity ratio of the 590 nm CT band and the 451 nm flavin band.

3). A plot of A_{610nm}/A_{455nm} (R_1), which represents the intensity ratio of the 610 nm band, characteristic of a CT, and the main flavin band at 455 nm, reaches a maximum at 3 equiv of NADPH (Figure 3).

The addition of 1.5 equiv/FAD of Cd(II) to the EH_2 form of GR has a very small effect on the absorption spectrum (not shown). In fact, preliminary experiments showed that Cd(II) concentrations equal to or higher than 4 equiv/FAD are necessary to observe a maximal perturbation of the absorption spectrum. Figure 2 shows two absorption spectra typical of the titration of GR with NADPH in the presence of 4.5 equiv of Cd(II). With reference to the positions of the flavin bands of EH_2, we observe a very small red shift of the 450 nm band (451 versus 450 nm) and a marked blue shift of its main shoulder (473 versus 479 nm) (Figure 2). These spectral alterations are thus clearly different from those detected for EH_2 in the presence of Hg(II) (Figures 1 and 2). The flavin bands are also different in terms of intensity with a small hyperchromic effect for EH_2 in the presence of Cd(II) (Figures 1 and 2). The 540 nm CT band is again absent but is replaced by a broad 590 nm band when 3−4 equiv of NADPH are added (Figures 2 and 3, Table 1). In fact, the evolution of R_2 that represents the intensity ratio of the 590 nm CT band and the 451 nm band (A_{590nm}/A_{451nm}) shows two parts when the NADPH concentration is increased. At low NADPH concentrations (1−3 equiv/FAD), the strong increase in R_2 indicates the formation of the 590 nm CT band (Figure 3). At higher concentrations of NADPH (3−14 equiv/FAD)); R_2 continues to significantly increase but this effect is due to a displacement of Cd(II) from the enzyme by the NADPH excess, allowing a partial restoration of the broad 540 nm CT band and thus an apparent increase in absorption at 590 nm. In other words, the Cd(II) ion bound to GR is easily transferred to free NADPH. This effect is less pronounced in the case of the EH_2-Hg(II) complex. The complexes of Hg(II) and Cd(II) with free NADPH are likely different in terms of coordination and stability and thus can explain the different behavior of the two metal ions. All these absorption data establish the reversibility of the Cd(II) and Hg(II) binding to EH_2 under anaerobic conditions.

RR Spectra of GR in the Presence of Hg(II) or Cd(II). In this RR study, the band numbering previously adopted for the prominent RR bands of oxidized flavoenzymes has been used (*16*, *23*−*26*). The assignments given in Table 2 have been discussed in a previous publication (*16*). The 1300−1670 and 1030−1300 cm^{-1} regions of the 441.6 nm excited RR spectra of oxidized GR are shown in Figures 4a and 5a. The addition to E_{ox} of up to 10 equiv/FAD of Hg(II) or Cd-(II) has no influence on the RR spectra (not shown).

When compared to the RR spectra of oxidized GR, those of the enzyme anaerobically reduced by NADPH exhibit significant positive shifts (2−7 cm^{-1}) for RR bands II, III, IV, V, and VI (Figure 4b). On the contrary, band VII is downshifted by 2 cm^{-1}. Band shifts are also detected for bands VIII, IX, X, XI, and XIII (Figure 5b). All these spectral changes were previously described using different Raman equipment (*16*). The concentration of NADPH (3−10 equiv/FAD) has no influence on the RR spectra of the EH_2-metal complexes excited at 441.6 or 363.8 nm (spectra not shown). The RR spectra of GR reduced by NADPH (3 equiv) in the presence of Hg(II) (1.5 equiv) or Cd(II) (4.5 equiv) are shown in Figures 4c,d and 5c,d. When compared to the spectrum obtained in the absence of metal ion, the frequencies of bands II, III, IV, V, and VI are downshifted by 3−6 cm^{-1} (Figures 4b and 5b). Band VII is upshifted by 2 cm^{-1}. In fact, the RR spectra of EH_2 in the presence of Hg(II) or Cd(II) strongly resemble the spectrum of E_{ox} (Figure 5a). However, the frequencies of bands II and III are significantly lower for the EH_2-metal complexes than for E_{ox} (1577 and 1542 cm^{-1} versus 1579 and 1545 cm^{-1}). Moreover, a shoulder on band VII is detected at 1338−1339 cm^{-1} (Figure 4c,d). In the 1050−1300 cm^{-1} region of the RR spectra, band VIII is observed at 1292 cm^{-1} for EH_2 in the absence or presence of heavy metal (Figure 5b,c,d). Similarly, band X maintains a significant contribution at 1265−1266 cm^{-1} for NADPH-reduced GR as well as for its forms inhibited by Hg(II) or Cd(II) (Figure 5b,c,d). However, a 1245−1246 cm^{-1} component remains active and is slightly downshifted when compared to that detected in the spectrum of E_{ox} (1248 cm^{-1}). On the contrary, the frequencies of bands IX (1275−1276 cm^{-1}), XI (1224−1225 cm^{-1}), XII (1180−1181 cm^{-1}), and XIII (1153−1154 cm^{-1}) are unaffected in the RR spectra of EH_2-Hg(II) and EH_2-Cd(II) relative to E_{ox} (Figure 5a,c,d).

DISCUSSION

Absorption Spectra. The absorption spectrum of E_{ox} is not modified by the addition of either Hg(II) or Cd(II). On the

Table 2: Observed Frequencies (cm^{-1}) of the RR Modes of Oxidized (E_{ox}) and NADPH-Reduced (EH_2) Forms of Yeast GR in the Absence or the Presence of Metal Ion

RR band[a]	E_{ox}	EH_2	EH_2 + Hg(II)	EH_2 + Cd(II)	assignment[b,c]	ring[c]
	1642	1641	1642	1643		
I	1629	1630	1630	1629	$\nu(C_8C_9)$, $\nu(C_9C_{9a})$	I
II	1579	1582	1577	1577	$\nu(C_{10a}N_1)$, $\nu(N_{10}C_{10a})$	III, II
III	1545	1547	1542	1542	$\nu(N_5C_{4a})$, $\nu(N_1C_{10a})$	II, III
IV	1498	1503	1500	1499	$\nu(N_5C_{4a})$, $\nu(N_{10}C_{9a})$	II
V	1460	1465	1462	1461	$\nu(C_7C_8)$, $\nu(C_8Me)$	I
	1451	1454	1450	1450		
VI	1403	1410	1404	1404	$\nu(N_3C_2)$, $\nu(N_1C_2)$	III
VII	1353	1351	1353	1353	$\nu(N_{10}C_{10a})$, $\nu(C_{5a}C_6)$	II, I
			1338	1339		
VIII	1297	1292	1292	1292	$\nu(N_5C_{5a})$, $\nu(C_8C_9)$	II, I
IX	1276	1279	1275	1275	$\nu(C_{4a}C_{10a})$, $\nu(C_4N_3)$	II, III
	1262	1265	1266	1266		
X					$\nu(N_3C_2)$, $\nu(N_3C_4)$	III
	1248	1247	1245	1246		
XI	1225	1230	1225	1224	$\nu(C_6C_7)$, $\nu(C_8Me)$	I
XII	1180	1186	1180	1181	$\nu(C_{4a}C_{10a})$, $\nu(C_4H_{4a})$	II, III, I
XIII	1154	1158	1153	1154	$\nu(C_7Me)$, $\nu(C_6H)$	I
	1144	1145	1143	1144		
	1132	1132	1133			
			1093	1092		
XIV	1059	1060	1059	1059	$\nu(N_3C_2)$, $\nu(N_1C_2)$	III

[a] Band numbering according to ref 23. [b] Mode assignment from refs 16 and 23−25. [c] See Figure 7 for atom and ring numberings.

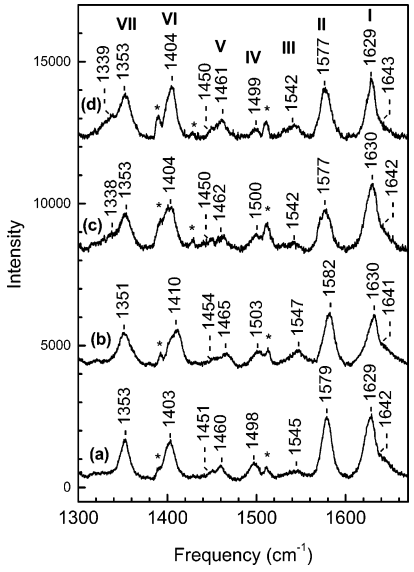

FIGURE 4: 1300−1670 cm^{-1} regions of RR spectra of yeast GR at pH 7.2. (A) Oxidized GR. (B) GR reduced with 3 equiv of NADPH. (C) GR in the presence of 1.5 equiv of Hg(II) and reduced with 3 equiv of NADPH. (D) GR in the presence of 4.5 equiv of Cd(II) and reduced with 3 equiv of NADPH. Excitation was 441.6 nm.

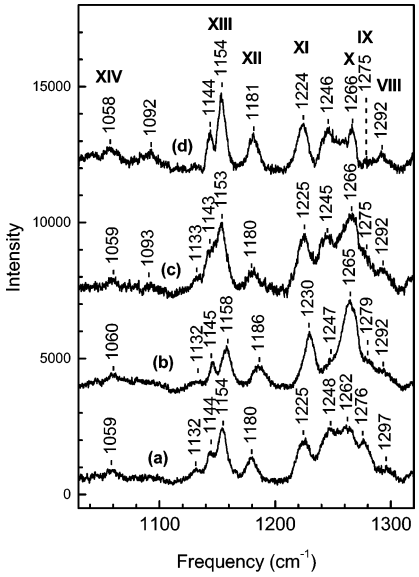

FIGURE 5: 1030−1320 cm^{-1} regions of RR spectra of yeast GR at pH 7.2. (A) Oxidized GR. (B) GR reduced with 3 equiv of NADPH. (C) GR in the presence of 1.5 equiv of Hg(II) and reduced with 3 equiv of NADPH. (D) GR in the presence of 4.5 equiv of Cd(II) and reduced with 3 equiv of NADPH. Excitation was 441.6 nm.

contrary, after two-electron reduction of GR by NADPH, the binding of heavy metal produces changes both in wavelength and in intensity for the main flavin bands as well as for the CT transition. When compared to the absorption spectrum of EH_2, the flavin bands of the EH_2−metal complexes are red-shifted. Moreover, these spectral shifts are metal-dependent (Table 1). The alteration of the $\pi \rightarrow \pi^*$ flavin transitions is indicative of a change in the structure and the environment of the isoalloxazine ring of FAD. As far as the CT transitions are concerned, the metal binding induces the disappearance of the characteristic 540 nm CT band of EH_2 (Table 1). This band is specific for a CT on the *si*-side of the flavin involving the proximal thiolate as an electron donor and the flavin isoalloxazine as an acceptor (*21*). In the spectrum of the EH_2−NADPH complex, the intensity of the 540 nm band is strongly increased. This hyperchromic effect was assigned to an additional CT on the *re*-side of the flavin between the bound NADPH acting as a donor and the flavin isoalloxazine acting as an acceptor (*22*). The crystal structure of the NADH complex of GR shows a parallel positioning of the isoalloxazine ring, the nicotinamide ring, and the phenol ring of a conserved Tyr residue (*8*). This spatial arrangment could be at the origin of the increased intensity of the 540 nm CT band. In the absorption spectra of the EH_2−metal complexes, the loss of the 540 nm band is thus primarily the consequence of a strong perturbation of the S^- (proximal thiolate)−FAD interaction (vide infra).

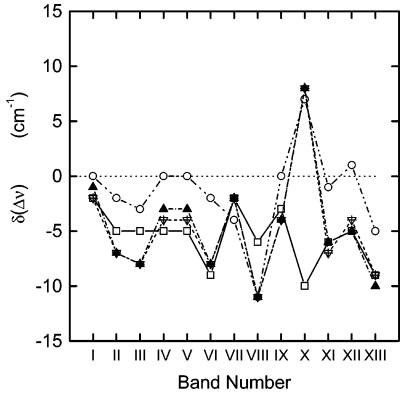

FIGURE 6: Raman diagrams of frequency shifts of the high-frequency modes (bands I−XIII) of the GR-bound FAD. The diagrams obtained for oxidized and NADPH-reduced GR are shown by open squares and open circles, respectively. Black triangles and reversed open triangles represent the diagrams obtained for GR reduced by NADPH in the presence of Hg(II) and Cd(II), respectively. The Raman data are listed in Table 2, and those of FAD in water are from Desbois et al. (*27*).

As far as the 590 or 610 nm band is concerned, it can be assigned to a CT band taking into account its wavelength as well as its intensity and width. On the one hand, this CT involves NADPH and not $NADP^+$ because it is observed with an NADPH excess. Under anaerobic conditions, only 1 equiv of $NADP^+$ is formed after E_{ox} reduction by NADPH. On the other hand, this CT involves the oxidized form of FAD. An excess of NADPH could reduce at least in part the FAD of the EH_2−metal complexes. However, the electronic transitions observed in the 400−500 nm region are clearly those of an oxidized FAD and are not modified by the addition of NADPH. Moreover, the Raman spectra give no indication of any flavin reduction. From these observations, we can exclude the formation of a number of possible CT between oxidized flavin and $NADP^+$ for the EH_2 form (i.e., FAD−$NADP^+$) as well as between reduced flavin and $NADP^+$ or NADPH for the four-electron reduced (EH_4) form (in particular, the $FADH^-$−$NADP^+$ CT). The 590 and 610 nm bands are thus assigned to FAD−NADPH CT. Its metal-dependent position suggests an extended CT from NADPH to the metal site (NADPH−FAD−metal/S^-).

RR Spectra. Table 2 summarizes the frequencies and assignments of the main RR bands observed in the spectra of the E_{ox} and EH_2 forms of GR, in the absence or the presence of heavy metal. To draw information about the protein effect on the isoalloxazine macrocycle, we used Raman diagrams plotting the frequency differences ν (flavoprotein) minus ν (flavin in water) ($\delta(\Delta\nu)$) of the Raman bands I−XIII as a function of this band number (*26*, *27*). The shape of the Raman diagram was associated with the electron distribution in the three rings of the isoalloxazine system; the direction of the shifts of $\delta(\Delta\nu)$ was related to the electron density at the macrocycle, a general positive shift corresponding to an increased electron density (*26*, *27*).

The diagrams drawn for the E_{ox} and EH_2 forms of GR in the absence of metal ion were previously discussed (*15*, *16*). They showed frequency shifts that are most frequently negative, indicating an electron-deficient isoalloxazine ring (Figure 6). Nevertheless, the diagram of EH_2, when compared to that of E_{ox}, exhibited an increased electron density through the entire isoalloxazine ring system, illustrating the influence

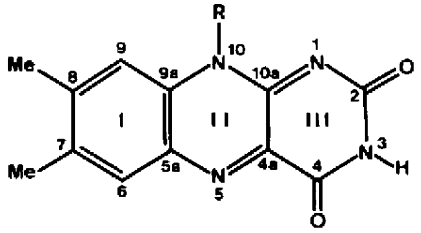

FIGURE 7: Chemical structure of the isoalloxazine ring of FAD.

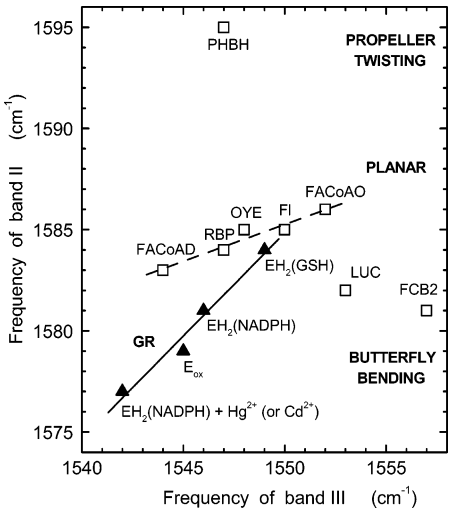

FIGURE 8: Plot of the observed band II frequency versus band III frequency of oxidized flavins and flavoproteins. The open squares represent the RR data obtained for fatty acyl-CoA dehydrogenase (FACoAD), riboflavin binding protein (RBP), old yellow enzyme (OYE), riboflavin, FAD and FMN (Fl), fatty acyl-CoA oxidase (FACoAO), *p*-hydroxybenzoate hydroxylase (PHBH), luciferase (LUC), and flavocytochrome b_2 (FCB2). The RR data are from Tegoni et al. (*26*) and Picaud and Desbois (*15*). The RR data obtained for GR are shown by black triangles.

of the disulfide reduction, and the subsequent formation of the CT complex between FAD and the proximal thiolate, on the isoalloxazine modes (*16*). In the case of the EH_2−metal ion complexes (Figure 6), the RR diagrams indicate an oxidized rather than an EH_2 form. The numerous negative shifts in the Raman diagram again indicate an electron deficiency throughout the isoalloxazine ring. This low electron density is approximately the same as that observed for the isoalloxazine ring of E_{ox}.

However, measurable differences in the frequencies of the RR bands II, III, VIII, and X are detected when the RR spectrum of E_{ox} is compared to that of EH_2 interacting with Hg(II) or Cd(II) (Table 2). Bands II and III were assigned to vibrational modes of the $N_1{=}C_{10a}{-}C_{4a}{=}N_5$ region (Figure 7), especially $N_1{-}C_{10a}$ and $C_{4a}{-}N_5$ stretches (*23*−*26*). The characterization of the frequencies of bands II and III has a particular importance, considering the involvement of the ring II−ring III junction in the functional properties of the flavins. The band II and III frequencies were found to be sensitive to the conformation of the isoalloxazine ring (*26*). A strict linear relationship was determined between the frequencies of bands II and III of planar isoalloxazine ring systems (*15*, *16*, *26*) (Figure 8). The points below the linear correlation were associated with a flavin ring adopting a bent conformation (*16*, *26*). Figure 8 plots the frequencies of bands II and III of E_{ox} and EH_2 in the absence or the presence of metal ion. The behaviors of the frequencies of bands II and

III of the GSH-reduced, NADPH-reduced, and oxidized GR were previously reported (*14*). The point corresponding to the frequencies of bands II and III of the NADPH-reduced enzyme in the presence of Hg(II) or Cd(II) (1577 and 1542 cm^{-1}, respectively) shows the most important deviation from the linear relationship previously determined for planar isoalloxazine rings (Figure 8). In fact, all the points corresponding to GR constitute a different linear relationship (Figure 8). This observation indicates that the isoalloxazine macrocycle distortion is of the same type but is increased from EH_2 reduced by GSH to EH_2 reduced by NADPH in the presence of Hg(II) or Cd(II). In the crystal structures of GR in its oxidized and NADH-reduced states, a small butterfly bent along the N_5-N_{10} axis of the flavin was determined (*7*). Figure 8 indicates a considerable increase in flavin bending when a metal ion is bound to EH_2 and illustrates a remarkable flexibility of the oxidized FAD cofactor in GR (*28*).

In addition to a sensitivity to flavin conformation, the frequency of band III was found to be affected by hydrogen bonding at the N_1/N_5 sites (*26*). In fact, the frequency of this mode is increased when the strength of the hydrogen bonding at N_5 (and N_1) is increased. As far as GR is concerned, the variation in band III frequency suggests a change in hydrogen bonding interaction at the N_5 site (*16*), presumably in relation with the conformational change of the flavin ring. The frequency of band III is downshifted when Hg(II) or Cd(II) is bound to EH_2, indicating a decreased H-bonding strength between the N_5(flavin) atom and a conserved Lys residue (Lys53 in yeast GR) (*10*). The isoalloxazine bending modifies the valence orbitals of N_5 and thus can weaken its H-bonding interaction with the Lys amino group.

Band X was assigned to a stretching mode of the N_3-C_4 and N_3-C_2 bonds. This band is sensitive to the H-bonding state of the N_3H site (*23*−*26*). On the basis of the observations made for oxidized GR, we attributed the 1248 cm^{-1} frequency to band X (*16*). Another component of band X was observed at 1261−1262 cm^{-1} in the RR spectra of E_{ox} (*16*). This latter component becomes major in the spectra of EH_2 generated by reduction with NADPH or GSH (*15*, *16*). The ca. 14 cm^{-1} upshift is indicative of a strengthening of the H-bond between the carbonyl group of the catalytic His residue (His456′ in yeast GR) and the N_3H group of the isoalloxazine ring (*16*). When the GR reduction by NADPH is performed in the presence of Hg(II) or Cd(II)), we observe a band X pattern, suggesting a mixed population of strong and weak N_3H(FAD)−CO(His) interactions, i.e., a strong H-bonding state (EH_2-like at 1266 cm^{-1}) and a weak H-bonding state similar to that observed for the major species of the E_{ox} spectrum (E_{ox}-like at 1245 cm^{-1}) (*16*). Therefore, the catalytic His residue that is paired with the distal redox thiol appears to be perturbed by the metal binding to EH_2.

Binding Site and Coordination State of the Metal Ion in GR. The absorption and RR data obtained in this study clearly establish that EH_2 is sensitive to the addition of Hg(II) or Cd(II); E_{ox} remains unchanged by the metal ion. The inhibition mechanism of GR by Hg(II) or Cd(II) is therefore initiated by the formation of a metal site in the EH_2 form. The redox dependence of the metal effect also indicates that the reductive half-reaction (eq 1) is not affected by the presence of metal ion. In addition, it shows that at least one redox site of GR is modified by the metal association, i.e., the isoalloxazine ring of FAD and the disulfide/dithiol center. The flavin ring is oxidized in both the E_{ox} and EH_2 states of GR (*15*, *16*). The maintenance of an oxidized state makes a direct binding of Hg(II) or Cd(II) to the isoalloxazine ring of FAD unlikely. Crystallographic studies on metalloflavin models showed that the N_4 and O_5 atoms of the isoalloxazine ring are the primary sites for metal coordination (*29*, *30*). Metal binding to the flavin ring produces steric and electronic effects that induce very important modifications in both absorption and RR spectra (*31*, *32*). We found no equivalence in the corresponding spectra of the EH_2-metal ion complexes. Finally, the crystal structures of GR show a conserved lysine residue interacting via H-bonds with the N_5 and O_4 sites of the flavin (Lys66 and Lys50 for human and *E. coli* GR, respectively). The placement of the side chain of this Lys residue appears to hinder any metal binding at N_5 and O_4. On the basis of the absorption and RR spectra as well as from the available X-ray structures of GR, a direct metal binding to the flavin is therefore excluded.

In contrast to the situation met for FAD, the oxidation state of the disulfide/dithiol center of GR is modified in the $E_{ox} \rightarrow EH_2$ transition. In oxidized GR, the active site cysteines are tied up as a disulfide and thus hardly available for metal coordination. The formation of EH_2 opens the disulfide redox center and forms a dithiol group. Because Hg(II) and Cd(II) have extremely high affinities for the sulfhydryls (*18*, *19*, *33*−*35*), the thiol/thiolate redox pair of reduced GR is an excellent site for metal binding.

Further support to this view comes from the analysis of our spectroscopic data. The electronic absorption spectra of EH_2 exhibit a specific broad band at 540 nm. This band is representative of a CT interaction between the thiolate group of the proximal Cys and the electron-deficient isoalloxazine ring (*16*, *21*, *22*). In the absorption spectra of the EH_2−metal complexes, the quenching of the Cys^-−FAD CT band (540 nm) is a key probe of the participation of the thiol/thiolate group of the proximal Cys in the Hg(II) or Cd(II) binding. In fact, the proximal and distal redox Cys share a single proton (*21*). The macroscopic pK_a ascribed to the proximal thiol is low (3.6−5.1), and that of the distal thiol is close to neutrality (7.1) (*21*), indicating that the two redox Cys of GR has a thiolate character at pH 7.2. Therefore, the proximal and distal Cys appear to be primary targets for the Hg(II) or Cd(II) ion. Given the high affinities of Hg(II) and Cd(II) for thiol and thiolate ligands, the vicinity of the proximal and distal redox Cys of reduced GR in fact offers two strong coordination sites for metal binding. In general, the affinity of the divalent metal ions varies as a function of preferential coordination geometry, ion size, liganding atoms, and charge effects. Additional ligand(s) originating from the protein or the solvent may be thus necessary to complete the metal coordination in GR.

It is well-known that Hg(II) and Cd(II) have very distinct coordination preferences. The most common coordination number of Hg(II) is two. These compounds are linear or close to linearity (*36*, *37*). Three- and four-coordinations were also observed but are less common than the two-coordinated state (*38*, *39*). On the contrary, Cd(II) prefers four- or six-coordination (*40*, *41*). Up to now, no linear Cd(II)−dithiolate complex was characterized (*40*). The ionic radii of Hg(II) and Cd(II) are dependent on the coordination number of the

metal ion (*42*). It increases from 83 to 110 and 116 pm for two-, four-, and six-coordinated Hg(II), respectively. As far as the Cd(II) ion is concerned, its radius varies from 92 pm for four-coordination to 109 pm in a six-coordinated complex. For a given coordination state, the ionic radius of Cd(II) is thus systematically smaller than that of Hg(II).

The biochemistry of Hg(II) is dominated by its extremely high affinity reaction for soft ligands such as thiols and thiolates (*35*). Like Hg(II), the Cd(II) ion is thiophilic. However, its binding affinity for thiol/thiolate ligands is lowered when compared to that of Hg(II) (*19*, *33*, *43*−*45*). The preference of group 12 metals such as Cd(II) and Hg(II) for N-donor groups such as imidazole, another soft ligand, is well-known (*46*). O-donor ligands can also bind these metal ions (*46*, *47*).

In the crystal structure of GR reduced by NADH, the distance between the sulfur atoms of the proximal and distal redox-active Cys is 3.7 Å (*8*). Considering this distance, local rearrangements of the polypeptide chain appear to be necessary to accommodate a difference in ionic radius of the Hg(II) and Cd(II) ion, a probable difference in coordination geometry, as well as differences in metal−ligand bond length.

The metal−S(thiolate) bond lengths are dependent on the coordination number, the shortest bond lengths being associated with the smallest coordination number. Considering typical Hg(II)−S and Cd(II)−S bond lengths of 2.3−2.5 and 2.5−2.6 Å, respectively, the through-space distance between the two redox S(Cys) atoms is clearly too small for a cation insertion yielding a linear S(Cys)−metal−S(Cys) arrangement. A stabilization of the metal binding to EH_2 would thus necessitate (i) an increased separation, i.e., by ca. 1 Å, of the redox S(Cys) atoms to allow a linear bidentate geometry or (ii) the intervention of additional metal ligands to form higher coordination states and thus change the ligand geometry.

An inspection of the available crystal structures of GR makes highly probable a participation of the imidazole group of the catalytic His as a third site for metal coordination. The perturbation of the RR band X supports this suggestion. The binding of the metal ion by the imidazole ring of the catalytic His can indirectly affect the H-bonding interaction between the flavin N_3H site and the carbonyl group of this His residue. In this line, lipoamide dehydrogenase, in which the active site is very homologous to that of GR, both in sequence and in 3-D structure, accommodates a site for Zn(II) (*48*, *49*). This metal site is formed by the dithiol redox group and the catalytic His. To satisfy both the preference of Hg(II) for a low coordination number and the preservation of the overall structure of the active site, the Hg(II) ion bound to reduced GR would also be three-coordinated with a trigonal Hg(II)$(S-Cys)_2(N-His)$ ligation. The bonding interaction of a secondary weak N(His) ligation could facilitate a marked deviation of the prefered linear geometry of the S(Cys)−Hg(II)−S(Cys) grouping and thus could maintain a S(Cys)−S(Cys) separation of ca. 4 Å.

Given the similar properties of Cd(II) and Zn(II), the Cd(II) ion can coordinate the redox thiol/thiolate pair and the catalytic His residue of GR like the Zn(II) ion in lipoamide dehydrogenase (*49*). However, the Cd(II) centers included in proteins are either four- or six-coordinated (*50*). Because the GSSG site in GR is relatively polar, one or three water molecule(s) can complete the coordination sphere of the GR-bound Cd(II) ion, forming an intramolecular Cd(II)$(S-Cys)_2(N-His)(H_2O)$ or Cd(II)$(S\text{-}Cys)_2(N\text{-}His)(H_2O)_3$ complex. The binding of water molecule(s) to the bound Cd(II) could participate in a stabilization of the Cd(II) binding in GR.

From our RR investigation, one can conclude that the binding of Hg(II) or Cd(II) to reduced GR produces the same extent of flavin bending (vide supra). However, the EH_2−Hg(II) and EH_2−Cd(II) complexes exhibit significant differences in absorption spectra and, thus, point to variations in the FAD microenvironment. Changes in π-stacking or H-bonding of the isoalloxazine ring or in hydrophobicity of the flavin pocket could account for a change in absorption spectrum. The identity of the RR spectra of the EH_2−metal complexes excludes any difference in either π-stacking of ring I or H-bonding of the polar N_1, O_2, N_3, O_4, N_5, and N_{10} sites of the isoalloxazine ring. Only a difference in solvent environment appears to be plausible to account for modifications in wavelength and intensity of the flavin and CT electronic transitions without any change in frequency of the RR modes. This effect can be directly related to different ligation states of the Hg(II) and Cd(II) complexes in GR, promoting different electrostatic effects on the isoalloxazine ring of FAD. Alternatively, different hydration states of the coordinated metal ion in GR could alter the network of the water molecules located in the *si*-side of the isoalloxazine ring, thus producing a local change in hydrophobicity. As judged by the blue-shifted flavin bands, the flavin-binding pocket becomes more hydrophobic upon substitution of Hg(II) by Cd(II).

Another point concerns the influence of metal binding on the flavin redox potentials of GR and particularly the redox couple involving the EH_2 and EH_4 forms. On the one hand, our RR experiments clearly show a bending of the isoalloxazine ring upon metal coordination. Such a deformation is known to decrease the redox potential of the flavins, stabilizing the fully reduced form. On the other hand, NADPH forms a CT complex with the GR-metal complexes, but we observe no reduction, even partial, of the EH_2 form by the nicotinamide ring. Therefore, the electrostatic effects due the metal association to GR appear to cause a negative shift of the redox potential of the FAD, canceling or overpassing the positive effect induced by the flavin distortion.

GR Inhibition and Enzyme Rescuing. Our absorption and RR data are consistent with the fact that the binding of heavy metal to GR has no influence on the reductive half-reaction (eq 1). In blocking the redox thiol/thiolate pair formed after reduction by NADPH, the inhibition of GR by heavy metal concerns the second half-reaction, i.e., the exchange reaction (eq 3). Therefore, the metal ions and GSSG essentially compete for the distal Cys of the EH_2 state.

In the frame of this study, we observed that Hg(II) and Cd(II) can be detoxified in the presence of an excess of NADPH under anaerobic conditions. In the presence of low concentrations of Hg(II) or Cd(II), NADPH thus acts as a chelator, decreasing the metal ion concentration available for the thiol/thiolate group of EH_2. As far as Hg(II) is concerned, it forms a 1:1 complex with NADPH. A K_d smaller than 10^{-9} M was estimated for this binding (*51*). Hg(II) and Cd(II) form strong complexes with GSH. Considering the high values for the association constants (*17*, *18*, *34*, *44*, *45*), we speculate that GSH can constitute a more

efficient chelator than NADPH. Therefore, under anaerobic conditions, GSH, and to a lesser degree, NADPH, can reverse the inhibition of GR by the heavy metals. In the cells, GSH is both a good carrier for Hg(II) or Cd(II) and an antioxidant by its reducing power. NADPH also has reducing properties and coordinates these metal ions. The enzyme has thus two means of reversing moderate metal ion inhibitions.

In vitro, a major problem concerns the presence of dioxygen when reduced GR and the metal ions are simultaneously present. All the experiments presented in this paper were done under anaerobic conditions. However, in the presence of atmospheric oxygen concentrations, we have observed that the EH_2−metal complexes produce an oxidized form of GR affected in absorption properties as well as in catalysis (data not shown). The exact nature of these oxidized species was not investigated. As a result of a Fenton-like reaction (*52*), reactive oxygen species were most probably formed when the EH_2−metal complexes were in contact with dioxygen.

CONCLUSION

The interaction of GR with Hg(II) and Cd(II) has been studied by absorption and RR spectroscopies. This investigation has clearly demonstrated that the two redox centers, the flavin and the redox-active disulfide/dithiol, are affected by the metal association. The point concerning the thiol/thiolate center acting as a target of metal ion binding is not unexpected considering most of the published data on flavoenzyme transhydrogenases. However, it is now firmly and directly established. A direct coordination of the metal ion to the thiol/thiolate groups of the redox Cys pair and the catalytic His thus constitutes a primary origin for the GR inhibition. As a consequence of metal binding, the flavin is also affected. These new results concern the conformation of the isoalloxazine ring by an increased butterfly bending as well as the microenvironment of the flavin that is modified.

Finally, the results of this study will be used as a comparative basis for similar absorption and RR studies on mercuric ion reductase, an enzyme closely related to GR in which an EH_2−Hg(II)−NADPH complex is a competent intermediate for reduction of Hg(II) into Hg(0).

REFERENCES

1. Brennan, R. J., and Schiestl, R. H. (1996) Cadmium is an inducer of oxidative stress in yeast, *Mutat. Res. 356*, 171−178.
2. Westwater, J., McLaren, N. F., Dormer, U. H., and Jamieson, D. J. (2002) The adaptative response of *Saccharomyces cerevisiae* to mercury exposure, *Yeast 19*, 233−239.
3. Ercal, N., Gurer-Orhan, H., and Aykin-Burns, N. (2001) Toxic metals and oxidative stress. Part I: mechanisms involved in metal-induced oxidative damage, *Curr. Top. Med. Chem. 1*, 529−539.
4. Meister, A. (1995) Glutathione metabolism, *Methods Enzymol. 251*, 3−7.
5. Inzé, D., and Van Montagu, M. (1995) Oxidative stress in plants, *Curr. Opin. Biotechnol. 6*, 153−158.
6. Williams, C. H., Jr. (1992) Lipoamide dehydrogenase, glutathione reductase, thioredoxin reductase, and mercuric ion reductase, A family of flavoenzyme transhydrogenases, in *Chemistry and Biochemistry of Flavoenzymes* (Müller, F., Ed.) Vol. 3, pp 121−211, CRC Press, Boca Raton, FL.
7. Karplus, P. A., and Schulz, G. E. (1987) Refined structure of glutathione reductase at 1.54 Å resolution, *J. Mol. Biol. 195*, 701−729.
8. Karplus, P. A., and Schulz, G. E. (1989) Substrate binding and catalysis by glutathione reductase as derived from refined enzyme: substrate crystal structure at 2 Å resolution, *J. Mol. Biol. 210*, 163−180.
9. Mittl, P. R., and Schulz, G. E. (1994) Structure of glutathione reductase from *Escherichia coli* at 1.86 Å resolution: comparison with the enzyme from human erythrocytes, *Protein Sci. 3*, 799−809.
10. Collinson, L. P., and Dawes, I. W. (1995) Isolation, characterization and overexpression of the yeast gene, GLR1, encoding glutathione reductase, *Gene (Amst.) 156*, 123−127.
11. Arscott, L. D., Veine, D. M., and Williams, C. H., Jr. (2000) Mixed disulfide with glutathione as an intermediate in the reaction catalyzed by glutathione reductase from yeast and as a major form of the enzyme in the cell, *Biochemistry 39*, 4711−4721.
12. Shigeoka, S., Onishi, T., Nakano, Y., and Kitaoka, S. (1987) Characterization and physiological function of glutathione reductase in *Euglena gracilis* z, *Biochem. J. 242*, 511−515.
13. Acan, N. L., and Tezcan, E. F. (1995) Inhibition kinetics of sheep brain glutathione reductase by cadmium ion, *Biochem. Mol. Med. 54*, 33−37.
14. Chrestensen, C. A., Starke, D. W., and Mieyal, J. J. (2000) Acute cadmium exposure inactivates thiotransferase (glutaredoxin), inhibits intracellular reduction of protein-glutathionyl-mixed disulfides, and initiates apoptosis, *J. Biol. Chem. 275*, 26556−26565.
15. Picaud, T., and Desbois, A. (2002) Resonance Raman characterization of the two-electron reduced forms of yeast glutathione, in *Flavins and Flavoproteins* (Chapman, S., Perham, R., and Scrutton, N., Eds.), pp 329−334, Rudolph Weber, Berlin.
16. Picaud, T., and Desbois, A. (2002) Electrostatic control of the isoalloxazine environment in the two-electron-reduced states of yeast glutathione reductase, *J. Biol. Chem. 277*, 31715−31721.
17. Carlberg, I., and Mannervik, I. (1977) Purification by affinity chromatography of yeast glutathione reductase, the enzyme responsible for the NADPH-dependent reduction of the mixed disulfide of coenzyme A and glutathione, *Biochim. Biophys. Acta 484*, 268−274.
18. Fuhr, B. J., and Rabenstein, D. L. (1973) Nuclear magnetic resonance studies of the solution chemistry of metal complexes. IX. The binding of cadmium, zinc, lead, and mercury by glutathione, *J. Am. Chem. Soc. 95*, 6944−6950.
19. Perrin, D. D., and Watt, A. E. (1971) Complex formation of zinc and cadmium with glutathione, *Biochim. Biophys. Acta 230*, 96−104.
20. Gomez de Gracia, A., Bordes, L., and Desbois, A. (2005) Spectroscopic Characterization of Hydroxide and Aqua Complexes of Fe(II)−Protoheme, Structural Models for the Axial Coordination of the Atypical Heme of Membrane Cytochrome b_6f, *J. Am. Chem. Soc. 127*, 17634−17643.
21. Sahlman, L., and Williams, C. H., Jr. (1989) Titration studies on the actives sites of pig heart lipoamide dehydrogenase and yeast glutathione reductase as monitored by the charge transfer absorbance, *J. Biol. Chem. 264*, 8033−8038.
22. Krauth-Siegel, R. L., Arscott, L. D., Schönleben-Janas, A., Schirmer, R. H., and Williams, C. H., Jr. (1998) Role of active site tyrosine residues in catalysis by human glutathione reductase, *Biochemistry 37*, 13968−13977.
23. Bowman, W. D., and Spiro, T. G. (1981) Normal mode analysis of lumiflavin and interpretation of resonance Raman spectra of flavoproteins, *Biochemistry 20*, 3313−3318.
24. Abe, M., and Kyogoku, Y. (1987) Vibrational analysis of flavin derivatives: normal coordinate treatments of lumiflavin, *Spectrochim. Acta 43A*, 1027−1037.
25. Lively, C. R., and McFarland, J. T. (1990) Assignment and the effect of hydrogen bonding on the vibrational normal modes of flavins and flavoproteins, *J. Chem. Phys. 94*, 3980−3994.
26. Tegoni, M., Gervais, M., and Desbois, A. (1997) Resonance Raman study on the oxidized and anionic semiquinone forms of flavocytochrome b_2 and L-lactate monooxygenase. Influence of the structure and environment of the isoalloxazine ring on the flavin function, *Biochemistry 36*, 8932−8946.
27. Desbois, A., Tegoni, M., Gervais, M., and Lutz, M. (1989) Flavin and heme structures in lactate:cytochrome c oxidoreductase: a resonance Raman study, *Biochemistry 28*, 8011−8022.
28. Lennon, B. W., Williams, C. H., Jr., and Ludwig, M. L. (1999) Crystal structure of reduced thioredoxin reductase from *Escherichia coli*: structural flexibility in the isoalloxazine ring of the flavin adenine dinucleotide cofactor, *Protein Sci. 8*, 2366−2379.
29. Garland, W. T., and Fritchie, C. J., Jr. (1974) Metalloflavoprotein models: the crystal structure of bis(riboflavin) bis(cupric perchlorate) dodecahydrate, *J. Biol. Chem. 249*, 2228−2234.

30. Yu, M. W., and Fritchie, C. J., Jr. (1975) Interactions of flavins with electron-rich metals. The crystal structure of bis(10-methylisoalloxazine) copper (I) perchlorate formic acid, *J. Biol. Chem. 250*, 946−951.
31. Clarke, M. J., Dowling, M. G., Garafalo, A. R., and Brennan, T. F. (1980) Structural and electronic effects resulting from metal-flavin ligation, *J. Biol. Chem. 255*, 3472−3481.
32. Benecky, M., Yu, T.-J., Watters, K. L., and McFarland, J. T. (1980) Metal-flavin complexation. A resonance Raman study, *Biochim. Biophys. Acta 626*, 197−207.
33. Stricks, W., and Kolthoff, J. M. (1953) Reactions between mercuric mercury and cysteine and glutathione. Apparent dissociation constants, heats, and entropies of formation of various forms of mercuric mercapto-cysteine and -glutathione, *J. Am. Chem. Soc. 75*, 5673−5681.
34. Casas, J. S., and Jones, M. M. (1980) Mercury(II) complexes with sulfhydryl containing chelating agents: stability constant inconsistencies and their resolution, *J. Inorg. Nucl. Chem. 42*, 99−102.
35. Cheesman, B. V., Arnold, A. P., and Rabenstein, D. L. (1988) Nuclear magnetic resonance studies of the solution chemistry of metal complexes. 25. $Hg(thiol)_3$ complexes of Hg(II)−thiol ligand exchange kinetics, *J. Am. Chem. Soc. 110*, 6359−6364.
36. Steele, R. A., and Opella, S. J. (1997) Structures of the reduced and mercury-bound forms of merP, the periplasmic protein from the bacterial mercury detoxification system, *Biochemistry 36*, 6885−6895.
37. Rosenzweig, A. C., Huffman, D. L., Hou, M. Y., Wernimont, A. K., Pufahl, R. A., and O'Halloran, T. V. (1999) Crystal structure of the Atx 1 metallochaperone protein at 1.02 Å resolution, *Struct. Folding Des. 7*, 605−617.
38. Church, W. B., Guss, J. M., Potter, J. J., and Freeman, H. C. (1986) The crystal structure of mercury-substituted poplar plastocyanin at 1.9-Å resolution, *J. Biol. Chem. 261*, 234−237.
39. Utschig, L. M., Wright, J. G., and O' Halloran, T. V. (1993) Biochemical and spectroscopic probes of mercury(II) coordination environments in proteins, *Methods Enzymol. 226*, 71−97.
40. Santos, R. A., Gruff, E. S., Koch, S. A., and Harbison, G. S. (1991) Solid-state ^{199}Hg and ^{113}Cd NMR studies of mercury− and cadmium−thiolate complexes. Spectroscopic models for [Hg-$(SCys)_n$] centers in the bacterial mercury resistance proteins, *J. Am. Chem. Soc. 113*, 469−475.
41. Li, Z.-S., Lu, Y.-P., Zhen, R.-G., Szczypka, M., Thiele, D., and Rea, P. A. (1997) A new pathway for vacuolar cadmium sequestration in *Saccharomyces cerevisiae*: YCF1-catalyzed transport of bis(glutathionato)cadmium, *Proc. Natl. Acad. Sci. U.S.A. 94*, 42−47.
42. Shannon, R. D. (1976) Revised effective ionic radii and systematic studies of interatomic distances in halides and chalcogenides, *Acta Crystallogr. A32*, 751−767.
43. Martell, A. E., and Smith, R. M. (1974) in *Critical Stability Constants*, Vol. 1, Plenum Press, New York.
44. Smith, R. M., and Martell, A. E., (1976) in *Critical Stability Constants*, Vol. 4, Plenum Press, New York.
45. Nielson, K. B., Atkin, C. L., and Winge, D. R. (1985) Direct metal-binding configurations in metallothionein, *J. Biol. Chem. 260*, 5342−5350.
46. Lippard, S. J., and Berg, J. M. (1994) in *Principles of Bioinorganic Chemistry*, University Science Books, Mill City, CA.
47. Ahrland, S., Chatt, J., and Davies, N. R. (1958) The relative affinities of ligand atoms for acceptor molecules and ions, *Q. Rev. 12*, 265−276.
48. Mattevi, A., Shuerbeck, A. J., and Mol, W. G. J. (1991) Refined crystal structure of lipoamide dehydrogenase from *Azotobacter vinelandii* at 2.2 Å resolution. A comparison with the structure of glutathione reductase, *J. Mol. Biol. 220*, 975−994.
49. Gazaryan, I. G., Krasnikov, B. F., Ashby, G. A., Thorneley, R. N. F., Kristal, B. S., and Brown, A. M. (2002) Zinc is a potent inhibitor of thiol oxidoreductase activity and stimulates reactive oxygen species production by lipoamide dehydrogenase, *J. Biol. Chem. 277*, 10064−10072.
50. Summers, M. F. (1988) ^{113}Cd NMR spectroscopy of coordination compounds and proteins, *Coord. Chem. Rev. 86*, 43−134.
51. Marshall, J. L., Booth, J. E., and Williams, J. W. (1984) Characterization of the covalent mercury(II)-NADPH complex, *J. Biol. Chem. 259*, 3033−3036.
52. Watanabe, M., Henmi, K., Ogawa, K., and Suzuki, T. (2003) Cadmium-dependent generation of reactive oxygen species and mitochondrial DNA breaks in photosynthetic and non-photosynthetic strains of *Euglena gracilis*. *Comp. Biochem. Physiol. Part C: Toxicol. Pharmacol. 134*, 227−234.

BI061304M